Isotope and element distributions of the evaporation residues from fusion of 160 MeV ^{32}S with ^{24,25,26}Mg and ^{27}Al

F. Pühlhofer* and W. F. W. Schneider
Gesellschaft für Schwerionenforschung GSI, Darmstadt, Germany

F. Busch
Sektion Physik der Universität München, Germany

J. Barrette,† P. Braun-Munzinger,‡ C. K. Gelbke,§ and H. E. Wegner¶
Max-Planck-Institut für Kernphysik, Heidelberg, Germany

(Received 24 May 1977)

Evaporation residues from fusion reactions induced by 160 MeV ^{32}S on targets of ^{24,25,26}Mg and ^{27}Al were identified by means of a time-of-flight ΔE-E detector telescope. Angular distributions were measured in the range from 3° to 16° and total yields were determined as a function of A and Z of the products. The mass distributions of the evaporation residues (summed over Z) show the typical structure arising from the competition between nucleon and α evaporation in the decay of the highly excited (83 to 90 MeV) compound nuclei, with only little variation between the four systems. It is concluded that the deexcitation mechanism is to a large extent independent of the individual structure of the nuclei in the decay chains. This is also demonstrated by the yield distributions for the individual nuclides, in particular by the similarity of the yield patterns obtained in the N-Z plane for the compound nuclei ^{59}Cu and ^{57}Ni. The data are reproduced very well by evaporation calculations based on the statistical theory. Effects of nuclear deformations due to the high angular momentum on the shape of the yrast line and on the transmission coefficients for the emitted light particles were included. The influence of shell effects in the level densities at high excitation was studied and found to be negligible above 15 MeV excitation.

[NUCLEAR REACTIONS ^{32}S on ^{24}Mg, ^{25}Mg, ^{26}Mg, ^{27}Al, E=160.7 MeV $\sigma(\theta,A,Z)$ for fusion products. Discussed systematics of nuclide distributions as function of compound-nucleus mass. Comparison with evaporation calculations, shell effects in level densities studied.]

I. INTRODUCTION

Direct identification of the evaporation residues from a fusion reaction by means of a detector telescope and measurement of the yields as a function of mass and atomic number of the products has proven to be a powerful method for studying the decay of highly excited compound nuclei. Recent advances in the detection techniques, in particular the improved resolution of time-of-flight telescopes, have made it possible to study compound systems as heavy as $A = 60$ in heavy-ion induced reactions. Examples of such experiments may be found in Refs. 1–4.

The main features of the data are well understood. The shape of the spectra and angular distributions of the evaporation residues was recognized as being characteristic for the decay mode of the compound nucleus, in particular for the number of α particles in the decay chain. The pronounced structure of the mass distribution and the typical distance of three mass units between relative maxima could be explained qualitatively as being due to the competition between emission of nucleons and α particles. The dependence of this structure on mass and excitation energy of the compound nucleus was studied. In most cases the evaporation residues were identified by their mass only. Apart from a few γ-spectroscopic studies there are few data on cross sections of individual nuclides. As far as the theoretical interpretation is concerned it could be shown[3–5] that the experimental results can be reproduced by means of a statistical evaporation model. One may therefore expect to obtain quantitative information about properties of nuclei at high excitation and angular momentum from such studies.

In this work, fusion reactions between 160 MeV ^{32}S and targets of ^{24}Mg, ^{25}Mg, ^{26}Mg, and ^{27}Al are discussed. In contrast to most of the earlier studies the evaporation residues were identified by mass and atomic number simultaneously by combining a ΔE-E and a time-of flight measurement. Particular emphasis is laid on studying the variation of the yield distributions under systematic variation of the compound nucleus in order to show to what extent the decay mechanism of a highly excited nucleus depends only on gross properties

of the product nuclei involved or on their microscopic structure. A detailed comparison with evaporation calculations is presented. In the theoretical analysis the influence of deformations on the deexcitation and of various assumptions concerning shell effects in nuclear level densities at high excitation are investigated. The latter point is of particular interest here, since the decay chains cross the shells $N=28$ and $Z=28$.

II. EXPERIMENTAL PROCEDURE

Self-supporting isotopically enriched targets of ^{24}Mg, ^{25}Mg, ^{26}Mg, and ^{27}Al of 400–500 μg/cm^2 thickness were bombarded with 160.7 MeV ^{32}S ions from the upgraded MP tandem accelerator of the Max-Planck-Institut für Kernphysik in Heidelberg. With dual foil strippers a beam of 10^{10} particles/s could be obtained on the target. Heavy reaction products were measured at angles between 3° and 16° using a time-of-flight ΔE-E detector telescope described previously.[6,7] A thin scintillator foil with a fast photomultiplier provided the start signal. The stop pulse as well as the energy signal were derived from a silicon detector at the end of a 1.80 m flight path. An ionization chamber in front of this detector measured the energy loss of the particles. The chamber had a grid-supported Parylene window of 30 μg/cm^2 thickness and was filled with 20 Torr pure isobutane gas.

For each event the energy E, the energy loss ΔE, and the time of flight T were recorded on magnetic tape. The data were analyzed utilizing the computer facilities of the Munich tandem laboratory. In a two-dimensional E vs ΔE plot the different elements could be identified unambiguously. The ΔE-E plane was covered with a net of polygons defining lines of constant Z. A one-dimensional Z spectrum was obtained by projecting the events along these lines. In the ET^2 vs E plane the different mass lines could clearly be assigned, but they showed a considerable energy dependent curvature due to pulse height defects in the silicon counter and due to the influence of the energy loss in the ΔE counter on the time-of-flight measurement. To avoid complicated analytical corrections, the same method as described above for the ΔE-E spectra was used for linearizing the data. Projections on the A and Z axes shown in Figs. 1 and 2 demonstrate the quality of the mass and Z resolutions obtained. The elements are very well separated. The mass spectra required unfolding by means of a multipeak Gaussian fitting program.

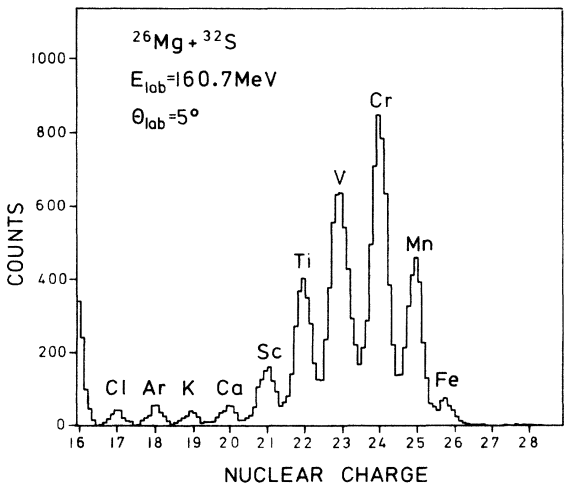

FIG. 1. Z spectrum of the evaporation residues from the reaction ^{32}S + ^{26}Mg at θ_{lab} = 5° obtained by projection of the linearized ΔE vs E data on the ΔE axis.

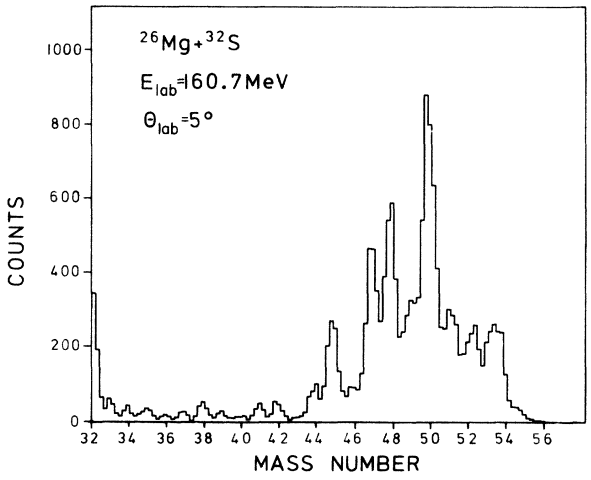

FIG. 2. Mass spectrum of the evaporation residues from reaction ^{32}S + ^{26}Mg at θ_{lab} = 5° obtained by projecting the linearized ET^2 vs E spectrum on the ET^2 axis.

Absolute differential cross sections were determined by comparing the evaporation residue yields to those for elastic scattering. The latter cross section scale was established by comparison to optical model calculations using parameters extrapolated from those of Gutbrod, Blann, and Winn.[8]

Typical angular distributions $d\sigma/d\theta = 2\pi \sin\theta \, d\sigma/d\Omega$ are shown in Fig. 3. Their maxima indicate the most probable deflection angle, which is related to the transverse momentum transferred to the residual nucleus by the evaporated particles. This deflection angle and the width of the angular distribution are characteristic of the number of α particles emitted from the compound nucleus.[4] The dependence on the number of evaporated neutrons and protons is weak.

The total yield for each evaporation residue was

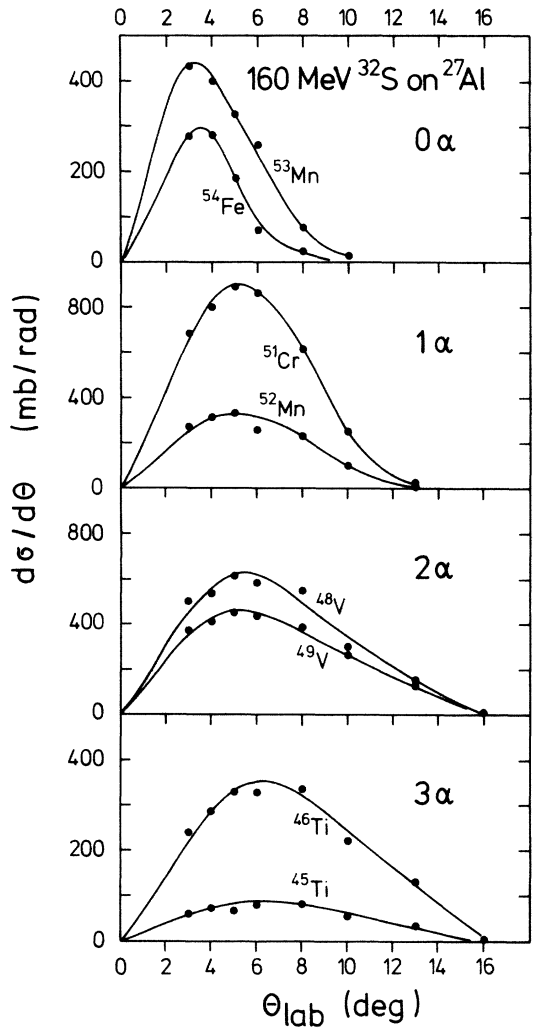

FIG. 3. Angular distributions of some representative fusion products in the reaction $^{32}S + ^{27}Al$. The shape of the distribution is characteristic of the number of α particles emitted in the decay chain. The solid lines are to guide the eye. Since the differential cross section $d\sigma/d\Omega$ is finite at 0°, the angular distributions should go through the origin.

determined by integrating the angular distributions. Relative errors are estimated to be about ±10% for the dominant isotopes, but are expected to be larger for the weaker ones. For the reaction $^{32}S + ^{24}Mg$, data were only taken at a single angle ($\theta = 6°$). Total cross sections were derived assuming the same shape of the angular distributions as for products with the same number of emitted particles in the reaction on ^{25}Mg.

The summed evaporation residue cross sections for the four reactions studied are given in Table I. Their accuracy is of the order of ±10%. The value for $^{32}S + ^{27}Al$ is consistent with the excitation functions given by Gutbrod, Winn, and Blann[9] and Kozub *et al.*[10] The cross sections in Table I represent only 50% of the reaction cross section calculated from the optical model. This indicated strong contributions of deep inelastic or other processes to the reaction cross section.

III. EXPERIMENTAL RESULTS

A. Mass distributions

It is instructive, in particular for the sake of comparison with previous results, to first discuss the mass distributions, which are obtained by summing the evaporation residue yields over the atomic number Z. They are shown in Fig. 4 for the four reactions investigated. Whereas the Z distributions (summed over A), which are included in Fig. 4, are featureless and obviously do not contain much information, the mass distributions exhibit pronounced structures. These structures, which are well known from earlier experiments, have been explained as being a consequence of the competition between the energetically approximately equivalent nucleon and α emission.[1-4] The assignments made in Fig. 4 between the peaks and the corresponding dominant decay chains (e.g., $4N1\alpha$ for emission of four nucleons and one α particle) are consistent with the energy balance of the reaction, the shape of the angular distributions (Fig. 3), and the results of evaporation cal-

TABLE I. Characteristics of the reactions studied.

160 MeV ^{32}S on	^{24}Mg	^{25}Mg	^{26}Mg	^{27}Al
Compound nucleus (CN)	^{56}Ni	^{57}Ni	^{58}Ni	^{59}Cu
Excitation energy $E_{x\,CN}$ (MeV)	82.8	87.4	90.0	86.7
Fusion cross section σ_{CN} (mb) (±10%)	860	820	840	870
Maximum angular momentum[a] L_0 ($\hbar$)	35.0	35.3	36.1	37.9

[a]Derived from σ_{CN}.

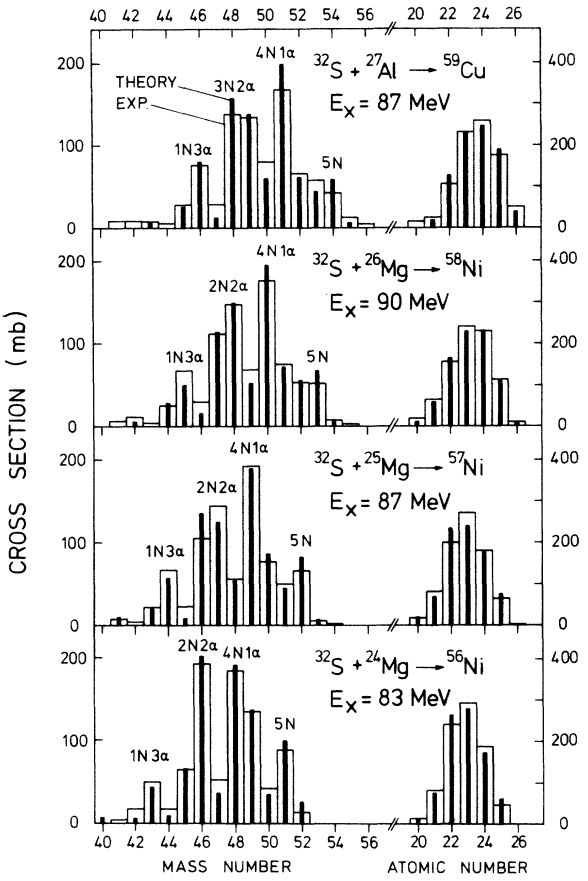

FIG. 4. Experimental and calculated evaporation residue cross sections. On the left the mass distributions (summed over Z) are shown, on the right the Z distributions (summed over A). The assignment of decay chains to the peaks in the mass distributions is discussed in the text. The solid bars represent results of statistical evaporation calculations (see Sec. IV A).

culations (Sec. IV). The average number of emitted particles varies between four and five in the dominant decay chains.

Except for a systematic shift by one mass unit corresponding to the variation of the compound nucleus mass, the shape of the mass distributions for the four systems is found to be very similar. This suggests that the deexcitation mechanism of the compound nucleus is to a large extent independent of the individual structure of the nuclei involved in the decay. This point will be discussed once more in connection with the nuclide distributions (see Sec. III B). The comparison with earlier data[4] for 130 MeV ^{32}S on ^{27}Al shows the expected change of the mass distribution due to the increase in the excitation energy of the compound nucleus (E_{xCN} = 72.6 → 86.7 MeV). On the other hand, one observes a striking similarity between the shape of the mass distribution for 160 MeV ^{32}S on ^{27}Al and that for 170 MeV ^{35}Cl on ^{27}Al[4] (the compound nucleus is ^{62}Zn), E_{xCN} = 88.9 MeV, L_0, the maximum angular momentum of the CN, is 44.6$\hbar$). The only difference is in the higher intensity of the $1N3\alpha$ peak in the ^{35}Cl-induced reaction. This is probably a consequence of the higher compound-nucleus spin in that reaction.

It was recognized earlier that the shape of evaporation residue mass distributions is strongly determined by the statistics of the decay process, which is one reason for the similarity of the distributions reported here and in earlier experiments. This observation suggests an attempt to describe these data by means of a very simple model. This can be done in the following way. The average number $\bar{n}$ of emitted particles is deduced from the initial compound-nucleus excitation energy E_{xCN} assuming a constant amount of energy needed for emitting a particle. This energy is found empirically to be about 18 MeV, therefore $\bar{n} = E_{xCN}/18$ MeV. The peaks in the mass distribution can then be assigned to the different combinations of nucleon and α emission in a n-particle decay chain. The relative intensity of the peaks is determined by the branching ratio between the decay modes. Because of their spin degrees of freedom, nucleons have a higher statistical weight, but this is compensated by the ability of α particles to remove larger amounts of angular momentum. Therefore we assume, on the average, equal probabilities for neutrons, protons and α particles ($\Gamma_n : \Gamma_p : \Gamma_\alpha = 1:1:1$). The cross section for a certain evaporation residue is then given by

$$\sigma(Z,A) = \sigma_{CN} \sum_n p(n)\, P(x,y,z;n)\, 3^{-n},$$

where $P(x,y,z;n) = n!/(x!y!z!)$ gives the number of permutations of x neutrons, y protons, and z α-particles that may lead to the same final nucleus ($x+y+z=n$). We included some variation of the number of emitted particles by introducing a

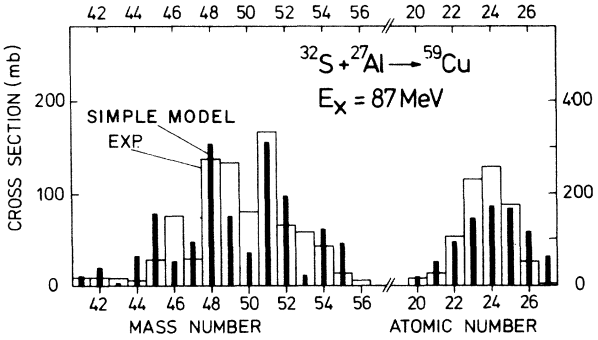

FIG. 5. Results of the simple compound-nucleus decay model described in Sec. III A (solid bars) in comparison with the measured evaporation residue yields for $^{32}S + ^{27}Al$.

a weight function $p(n)$ represented by a triangle function of half-width 1.6 centered around the mean value $\bar{n}$. The parameters mentioned were found empirically by comparison with several experimental mass distributions. The result of this calculation is shown for the case of 160 MeV ^{32}S on ^{27}Al in Fig. 5. The comparison to the other mass distributions looks very similar. In view of the crude approximations made the agreement is remarkable. However, it should be emphasized that this model is only a simple means to explain the statistical origin of the structure in the mass distributions. It does not reproduce nuclide distributions. It also introduces an arbitrary branching ratio $\Gamma_n : \Gamma_p : \Gamma_\alpha$, which cannot be justified at all within the framework of this model. This ratio represents an effective value, averaged over all excitation energies, spins, and nuclei in the decay chains, and it is known that it varies by orders of magnitude as a function of these variables. For a consistent description much more detailed evaporation calculations are necessary. They will be discussed in Sec. IV.

B. Nuclide distributions

The cross sections for the individual evaporation residues in the reactions investigated here are shown in Fig. 6 as a function of A and Z. From the mass distributions and their dependence on only the mass of the compound nucleus one learns that the number of emitted particles is more important than their charge. Therefore it seems reasonable to plot Z spectra for given mass numbers. In the other possible display mode (mass distributions for given Z) the data would only show little systematic trends when comparing the different reactions. Except for a possible influence of the individual level structure of the residual nuclei there are two effects that are expected to determine the Z distributions: the Q values for the decays and the Coulomb barrier with its influence on charged particle emission. Therefore, there will always be a tendency to adjust the ratio of emitted neutron and protons in the decay chains such that the residual nuclei lie close to the valley of stability, but somewhat on the neutron-deficient

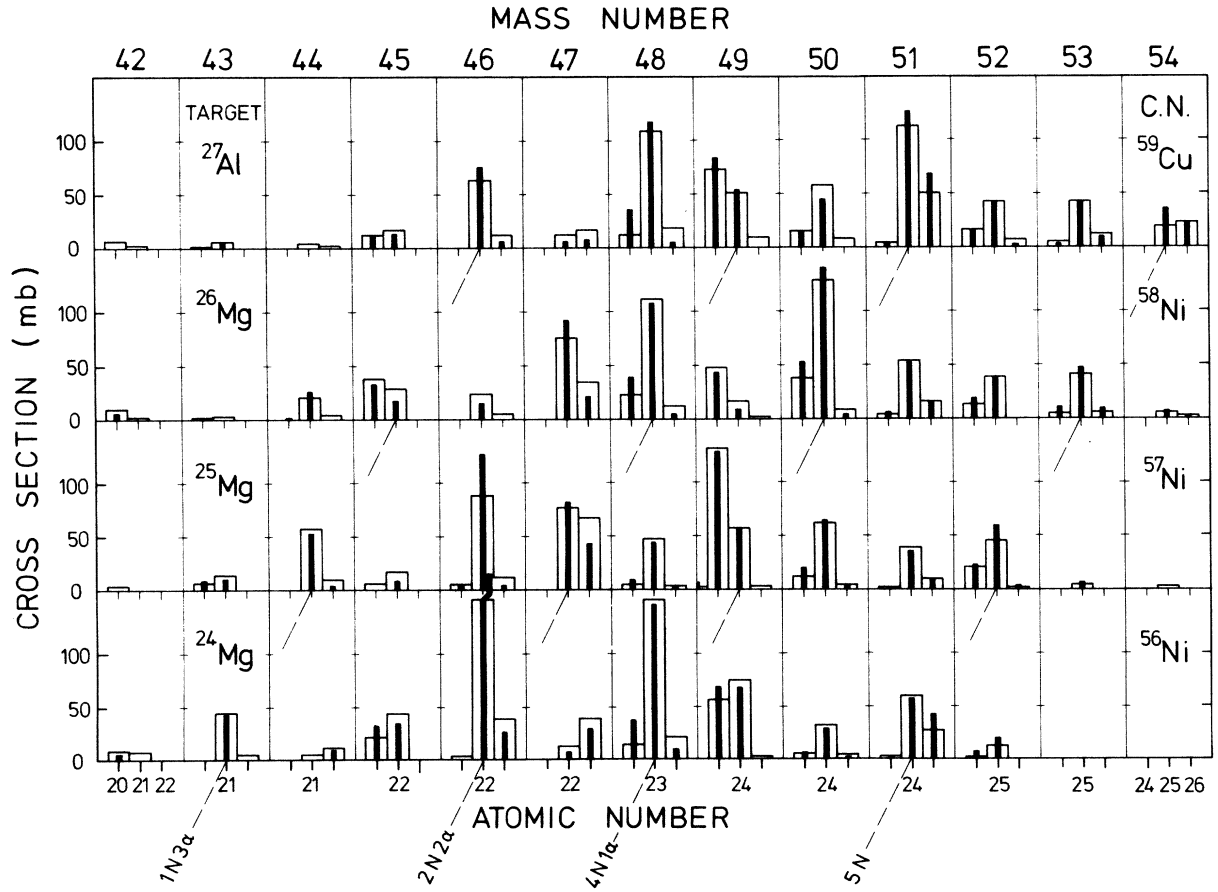

FIG. 6. Nuclide distributions of the evaporation residues. Each horizontal row belongs to one reaction. The solid bars represent results of statistical evaporation calculations (Sec. IV A). This figure corresponds to Fig. 4.

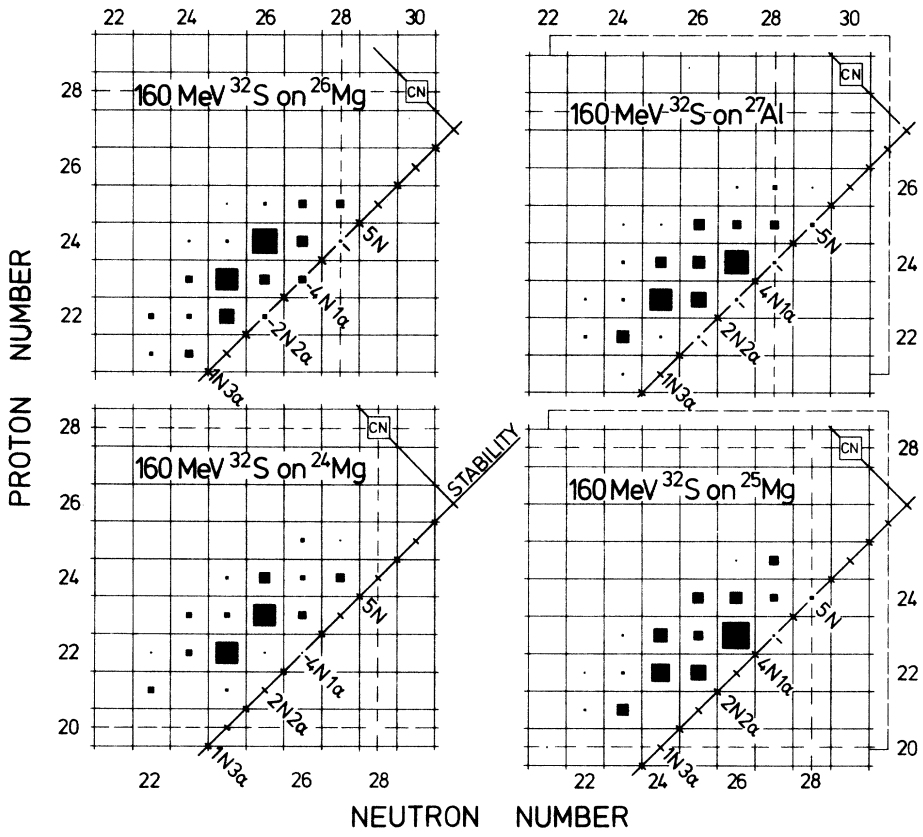

FIG. 7. Nuclide distributions of the evaporation residues. The side dimensions of the solid squares are proportional to the experimental cross sections. The purpose of these plots is to demonstrate the similarity of the intensity patterns obtained for different reactions. The suitable reference frame for comparison is the titled coordinate system indicated. One axis measures the mass evaporated from the compound nucleus, the other one the distance from the center of the valley of stability, which is close to the 45° line. The right-hand part of the figure containing the odd-mass compound nuclei is shifted intentionally so that the origin of the new reference frame is at the same location with respect to the upper right corners of each plot.

side due to the Coulomb barrier for protons. This means that the influence of the proton-neutron ratio of the compound nucleus on the element distribution of the residues is strongly reduced, except for multiple α decays, where the number of simultaneously emitted nucleons is small. These statements are seen to be consistent with the data shown in Fig. 6. There, one observes that for a given mass number A the relative intensities for different elements are fairly independent of the reaction. Close inspection reveals some dependence on the N/Z ratio of the compound nucleus.

One notes in Fig. 6 that the experimental nuclide distributions due to the decay of ^{59}Cu and ^{57}Ni are very similar except for a shift by two mass units including one Z unit. In order to demonstrate this more clearly the same data are shown in Fig. 7 in nuclidic chart presentation. One observes that the residue distributions essentially move parallel to the valley of stability corresponding to the change of the compound-nucleus mass. This is understood from the arguments made above. The similarity of the patterns obtained for ^{59}Cu and ^{57}Ni is, at first, somewhat surprising in view of the fact that for a given decay chain an even-even decay product nucleus in the former case corresponds to an odd-odd one in the latter, and vice versa. It is, however, well known that at a few MeV of excitation the level densities of both kinds of nuclei are very similar, if one refers to an energy scale which is shifted by twice the pairing energy Δ in one of the nuclei. The same pairing energy also affects the ground state Q values, with the result that both effects cancel. This means that for a given kinetic energy of the emitted particle, regions with identical level density are reached in the odd-odd as well as in the even-even product.

The similarity of the evaporation residue distributions in the N, Z plane in case of the reactions

on ^{25}Mg and ^{27}Al is due to the fact that the compound nuclei have very similar excitation energies and angular momenta in both reactions, and that they are only shifted parallel to the valley of stability, whose shape is the dominant factor in determining the final isotope and element distribution.

The discussion emphasizes once more what has already been concluded in Sec. III A, namely, that the deexcitation process is governed by average nuclear properties. The data can be explained entirely without referring to an influence of the individual structure of the nuclei involved in the decay. One reason for this is that most of the decays take place at rather high excitation energy. In addition, there is an averaging over a rather wide region in excitation and angular momentum in each decay step. However, one could think of cases where a single low-lying high-spin state attracts an appreciable cross section and where the microscopic structure of a nucleus must therefore be important.

IV. EVAPORATION CALCULATIONS

A. Assumptions and results

Mass distributions of evaporation residues in heavy-ion induced fusion reactions have successfully been described[3-5] by means of the statistical theory for compound-nucleus reactions. In this theory, it is assumed that a highly excited compound nucleus is formed which decays by successive evaporation of several light particles. Emission of neutrons, protons, α particles, and γ rays seem to be the only decay modes which have to be taken into account. Relative decay probabilities are calculated from the Hauser-Feshbach formula using transmission coefficients as given by the optical model with average parameters and level densities based on a Fermi gas model with individ-

TABLE II. Parameters for the evaporation calculations. Nomenclature as in Ref. 5.

Angular momentum distribution in the compound nucleus
Max. angular momentum L_0 derived from σ_{CN} (Table I)
diffuseness $d = 3.5\hbar$
Optical potentials for emitted particles [a]
Neutrons, Wilmore and Hodgson (Ref. 16)
Protons, Perey (Ref. 17)
α particles, Huizenga and Igo (Ref. 18)
γ-decay strengths [b]
$\xi(E1) = 0.5 \times 10^{-7} = 0.005$ W.u. (Weisskopf units)
$\xi(M1) = 0.5 \times 10^{-7} = 0.5$ W.u.
$\xi(E2) = 0.3 \times 10^{-8} = 20$ W.u.
Level density parameters
Region I ($E_x \lesssim 3$ MeV)
Discrete levels as far as known experimentally
Region II (3 MeV $\lesssim E_x \lesssim$ 10 MeV)
Fermi gas level density formula (Ref. 19) with empirical a and Δ from Dilg *et al.* (Ref. 13)
Effective moment of inertia $\mathcal{I} = 0.95\mathcal{I}_{rigid}$ (or $r_0 = 1.20$ fm)
Known high-spin states (Ref. 20) included as yrast levels
Region III ($E \gtrsim 15$ MeV) [c]
Fermi gas level density [d]
Level density parameters $a_{LDM} = A/8.5$ MeV^{-1}
Moment of inertia for rigid body
Radius parameter $r_0 = 1.28$ fm (Ref. 22)
Deformation from liquid-drop theory
Deformability $\delta = 10^{-4}$ [e]

[a] Radius parameter multiplied by 1.10 to take into account deformation (see text).

[b] These strengths are somewhat larger than average values derived from low-lying transitions (Ref. 23).

[c] The level density parameters are linearly interpolated between regions II and III.

[d] The virtual ground state is calculated using a liquid-drop ground state without shell and pairing corrections (Ref. 21).

[e] Used to calculate the effective moment of inertia $\mathcal{I} = \mathcal{I}_{sphere}(1 + \delta L^2)$.

ual empirical or average parameters, depending on the excitation energy. The application of this theory to the reactions under consideration is described extensively in Ref. 5. The following calculations are based on the formalism given there.

Results of calculations obtained by using the computer code CASCADE [5] are presented in Figs. 4 and 6 in comparison with the experimental data. The structure of the mass distributions (Fig. 4) is described very well. In particular, the ratio between nucleon and α emission, which is interesting because of its strong dependence on angular momentum, is reproduced by the theory. A slight deviation occurs only for the $1N3\alpha$ decay chain, the intensity of which is somewhat underestimated. As can be observed from Fig. 6, the agreement between theory and experiment also holds for the individual nuclides. The parameters used for these calculations are compiled in Table II. They were chosen in accordance with the policy described in Ref. 5. Many parameters can be determined empirically from independent experimental information, at least within certain limits. For some others, as the level densities at high excitation (liquid-drop region), estimates can only be obtained from theoretical models. The main uncertainties concern the extrapolation of γ strengths and transmission coefficients for the emitted particles, both obtained empirically for nuclei near or in their ground state, to high excitation energies. The same is true for the level densities. This latter point will be discussed later.

It was observed that it is important to modify the empirical parameters of the optical model used to generate transmission coefficients for the light particles in order to obtain the right balance between the intensities of pure nucleon and multiple α emission in the mass distributions. The major part of the decay takes place at relatively high angular momentum of the emitting nucleus ($20-30\hbar$). Based on the predictions of the liquid-drop model,[11] one assumes deformations of the rotating nucleus when calculating the yrast line and the spin dependence of the level densities. Therefore it is consistent to use also deformed potentials for the light particles. The effect of the deformation was simulated by using an increased potential radius. This assumption is suggested from the classical picture of a rotating nucleus, which emits particles in a plane perpendicular to the spin direction. An increase of 10% in the potential radius provided the correction needed to properly fit the mass distributions. It is difficult to justify this value quantitatively. According to the liquid-drop model[11] a nucleus with mass 60 and spin $30\hbar$ would be in a transition region between oblate and triaxial prolate deformation. Its deformation would, in the prolate case, correspond to an increase of the long axis by 20%, or, in the oblate case, to an increase of the radius perpendicular to the spin direction by 5%. In addition to this there may be an increase of the diffuseness of the potential, which would have a influence similar to the radius change. Such an effect was predicted for nuclei at higher temperatures by Sauer, Chandra, and Mosel.[12] Thus, our modification of the optical potentials is consistent with theoretical estimates. It leads to a lowering of the Coulomb barrier and therefore to a relative enhancement of α-particle emission. The effect on the calculated mass distribution consists in a decrease of the cross sections near the $5N$ peak by 20% and a corresponding increase of the $1N3\alpha$ and $3N2\alpha$ decay chains. It should be noted that this effect is completely different from that obtained by varying the shape of the yrast line. The latter would mainly redistribute the cross section within the multiple α decays.

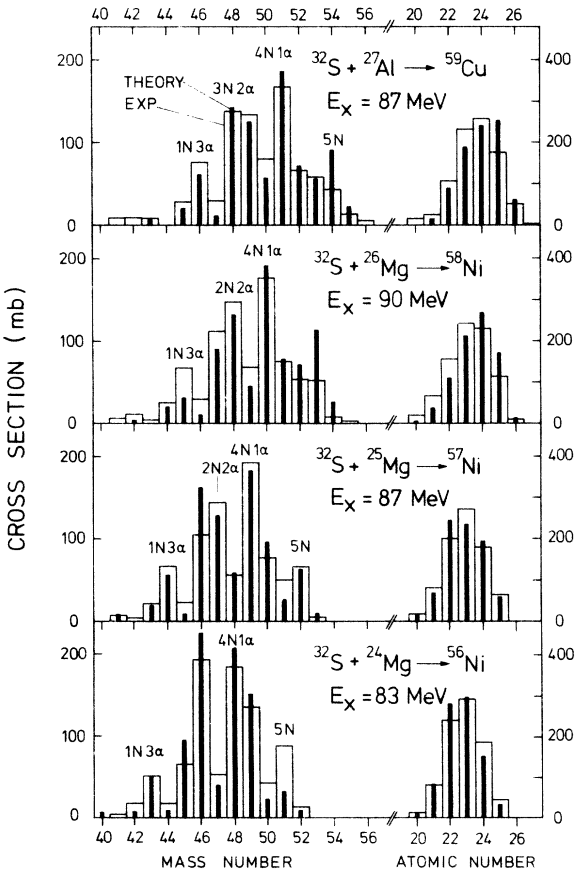

FIG. 8. Comparison between evaporation calculations (solid bars), in which shell effects in the level densities were assumed to persist over the whole excitation energy range (see Sec. IV B), with the experimental data. One notices strong deviations for the $5N$-decay chains.

This investigation shows that detailed evaporation calculations can reproduce the nuclide distributions of the evaporation residues very accurately, including the deviations from the systematic trends in individual cases. Except for the discussed modification of the optical potential for the emitted particles, the parameters used in the calculation are not seriously different from the ones estimated before. In view of the large number of parameters and because of the fact that such calculations need much computer time, it is very difficult to show that the parameters are determined uniquely by the fit to the data. However, the parameter set used seemed to be clearly the best one among about 17 sets in which the parameters ξ_L, L_0, d, r_0, $r_{0\mathrm{LDM}}$, δ, a_{LDM}, and the optical potentials were varied.

B. Shell effects in the level densities

As seen in Fig. 7, the decay chains of the compound nuclei cross the shells $N=28$ and $Z=28$. This fact suggests use of these reactions for a study of shell effects in the nuclear level densities at high excitation energy. This can be done by investigating their influence on the calculated mass and element distributions of the evaporation residues. In the vicinity of shell closures the level densities are reduced appreciably at low excitation energy (0–10 MeV). This can be observed in the level density parameters a and Δ determined empirically.[13] Based on theoretical predictions,[14,15] we assumed in our calculations that above a given excitation energy $U_{\mathrm{LDM}} = E_{x\mathrm{LDM}} - \Delta = 15$ MeV the shell effects disappear and the parameter a as well as the position of the virtual ground state defined by the parameter Δ assume values which depend smoothly on the mass number A (liquid-drop parameters, see Table II and Ref. 5).

In the calculations presented in Figs. 8 and 9 the extreme assumption was made that the level density parameters a and Δ determined empirically at low excitation energy are valid over the whole excitation range, i.e., that the shell effects persist up to the compound-nucleus excitation energies of about 80 to 90 MeV. One observes from the mass distributions shown in Fig. 8 that this assumption is inconsistent with the data. The disagreement is particularly striking for the $5N$ decay chain. Since the effect is opposite in different reactions it seems to be excluded that it can be compensated by changes in other parameters. One expects that the deviations can be seen more clearly in the nuclide distributions. Indeed, one observes from Fig. 9 that the ratio between the yields for different elements of a given isobar reacts sensitively even in cases in which there is only a small influence in the mass distribution (e.g., for $A=49$). The effect can partially be attributed to changes in the first emission step. In the reactions

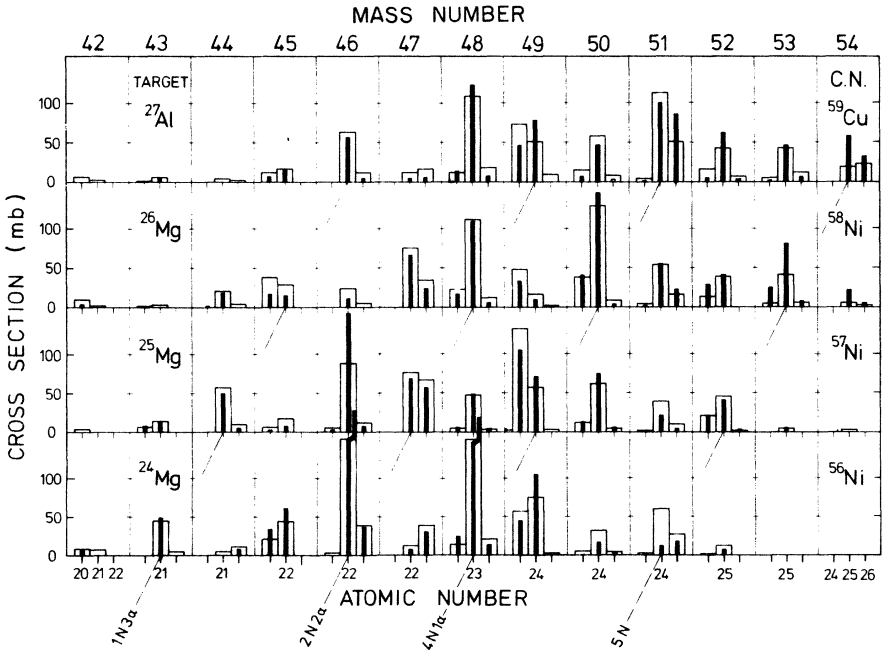

FIG. 9. Same as Fig. 8, but nuclide distributions. Note, for example, the deviation between theory and experiment in the element distribution for $A=49$ in the case of $^{32}S+^{27}Al$, where the mass spectrum shows no effect.

on ^{27}Al and ^{26}Mg α decay of the compound nucleus leads to semimagic products and is therefore reduced compared to nucleon emission, if shell effects were present at high excitation. The opposite holds for the reaction on ^{24}Mg.

These results can be taken as evidence for the predicted disappearance of shell effects in the level densities at higher excitation energies. If the transition energy is assumed to be 40 MeV, as predicted theoretically,[15] the deviation of the calculated cross section for the $5N$-decay chain from the standard calculation (using $U_{\mathrm{LDM}} = 15$ MeV, see Fig. 4) would be half the deviation shown in Fig. 8 (where $U_{\mathrm{LDM}} > 90$ MeV) for the case ^{32}S+^{27}Al, and very small in the other reactions. One may therefore conclude that the transition energy U_{LDM}, above which shell effects in the level densities disappear, lies between 15 and 40 MeV, with some preference for the smaller value. As was noted previously,[5] high excitation energy is automatically correlated with high angular momentum in these heavy-ion reactions, and the relatively low transition energy may therefore also be a consequence of deformations of the nucleus.

V. CONCLUSION

We have studied the decay chains of four different neighboring nuclei, ^{59}Cu, ^{58}Ni, ^{57}Ni, and ^{56}Ni at high excitation energy and angular momentum formed by the fusion of 160 MeV ^{32}S with the appropriate targets. It is shown that to a large extent the deexcitation process is independent of the microscopic structure of the nuclei involved. Evaporation calculations based on the statistical theory using the code CASCADE reproduce detailed features of the nuclide distributions and indicate that at high excitation energies shell effects do not influence the decay pattern. More important is the shape of the particle-emitting nuclei. Agreement between experiment and theory could only be obtained by increasing the potential radii of the highly excited nuclei by 10%, consistent with theoretical estimates of the rotating liquid-drop model.

---

*On leave from Fachbereich Physik, Universität Marburg, Germany.
†Present address: Brookhaven National Laboratory, Upton, New York 11973.
‡Present address: State University of New York at Stony Brook, Stony Brook, New York 11790.
§Present address: Lawrence Berkeley Laboratory, University of California, Berkeley, California 94720.
¶Senior U. S. Scientist Awardee of the Alexander von Humboldt Foundation, partially supported by the U.S.E.R.D.A. Permanent address: Brookhaven National Laboratory, Upton, New York 11973.

[1]F. Pühlhofer, W. Pfeffer, B. Kohlmeyer, and W. F. W. Schneider, Nucl. Phys. A244, 329 (1975).
[2]J. D. Garrett, H. E. Wegner, T. M. Cormier, E. R. Cosman, and A. J. Lazzarini, Phys. Rev. C 12, 481 (1975).
[3]A. Weidinger, F. Busch, G. Gaul, W. Trautmann, and W. Zipper, Nucl. Phys. A263, 511 (1976).
[4]T. M. Cormier, E. R. Cosman, A. J. Lazzarini, H. E. Wegner, J. D. Garrett, and F. Pühlhofer, Phys. Rev. C 15, 654 (1977).
[5]F. Pühlhofer, Nucl. Phys. A280, 267 (1977).
[6]A. Gamp, W. Bohne, P. Braun-Munzinger, and C. K. Gelbke, Nucl. Instrum. Methods 120, 281 (1974).
[7]J. Barrette, P. Braun-Munzinger, and C. K. Gelbke, Nucl. Instrum. Methods 126, 181 (1975).
[8]H. H. Gutbrod, M. Blann, and W. G. Winn, Nucl. Phys. A213, 285 (1973).
[9]H. H. Gutbrod, W. G. Winn, and M. Blann, Nucl. Phys. A213, 267 (1973).
[10]R. L. Kozub, N. H. Lu, J. M. Miller, D. Logan, T. W. Debiak, and L. Kowalski, Phys. Rev. C 11, 1497 (1975).
[11]S. Cohen, F. Plasil, and W. J. Swiatecki, Ann. Phys. (N.Y.) 82, 557 (1974).
[12]G. Sauer, H. Chandra, and U. Mosel, Nucl. Phys. A264, 221 (1976).
[13]W. Dilg, W. Schantl, H. Vonach, and M. Uhl, Nucl. Phys. A217, 269 (1973).
[14]V. S. Ramamurthy, S. S. Kapoor, and S. K. Kataria, Phys. Rev. Lett. 25, 386 (1970).
[15]F. C. Williams, G. Chan, and J. R. Huizenga, Nucl. Phys. A187, 225 (1972).
[16]D. Wilmore and P. E. Hodgson, Nucl. Phys. 55, 673 (1964); P. E. Hodgson, Annu. Rev. Nucl. Sci. 17, 1 (1967).
[17]F. G. Perey, Phys. Rev. 131, 745 (1963).
[18]J. R. Huizenga and G. Igo, Nucl. Phys. 29, 462 (1961).
[19]D. W. Lang, Nucl. Phys. 77, 545 (1966).
[20]W. Kutschera, Technische Universität München (private communication).
[21]W. D. Myers and W. J. Swiatecki, Nucl. Phys. 81, 1 (1966); Ark. Fys. 36, 343 (1967).
[22]W. D. Myers, Nucl. Phys. A204, 465 (1973).
[23]F. Bertrand, M. Martinot, and N. Verges, in *Nuclear Data in Science and Technology*, (International Atomic Energy Agency IAEA-SM-170/60, Vienna, 1973), Vol. II.